

Thermally induced mechanical and permeability changes around a nuclear waste repository – a far-field study based on equivalent properties determined by a discrete approach

Ki-Bok Min¹, Jonny Rutqvist², Chin-Fu Tsang² and Lanru Jing¹

¹Engineering Geology and Geophysics Research Group, Royal Institute of Technology (KTH), Stockholm, Sweden

²Earth Sciences Division, Lawrence Berkeley National Laboratory (LBNL), Berkeley, CA, USA

Abstract: A numerical investigation is conducted on the impacts of the thermal loading history on the evolution of mechanical response and permeability field of a fractured rock mass containing a hypothetical nuclear waste repository. The geological data are extracted from the site investigation results at Sellafield, England.

A combined methodology of discrete and continuum approaches is presented. The results of a series of simulations based on the DFN-DEM (Discrete Fracture Network-Distinct Element Method) approach provide the mechanical and hydraulic properties of fractured rock masses, and their stress-dependencies. These properties are calculated on a representative scale that depends on fracture network characteristics and constitutive models of intact rock and fractures. In the present study, data indicate that the large scale domain can be divided into four regions with different property sets corresponding to the depth. The results derived by the DFN-DEM approach are then passed on to a large-scale analysis of the far-field problem for the equivalent continuum analysis.

The large-scale far-field analysis is conducted using a FEM code, ROCMAS for coupled thermo-mechanical process. The results show that the thermal stresses of fractured rock masses vary significantly with mechanical properties determined at the representative scale. Vertical heaving and horizontal tensile displacement are observed above the repository. Observed stress and displacement fields also shows significant dependency on how the mechanical properties are characterized. The permeability changes induced by the thermal loading show that it generally decreases close to the repository. However, change of permeability is small, i.e., a factor of two, and thermally induced dilation of fracture was not observed. Note that the repository excavation effects were not considered in the study.

The work presented in this paper is the result of efforts on a benchmark test (BMT2) within the international co-operative projects DECOVALEX III and BENCHPAR.

1. Introduction

For many countries concerned about the safe isolation of nuclear wastes from the biosphere, disposal in a deep geological formation is considered an attractive option [1]. The intention of such disposal is to provide sufficient isolation, both from human activity and

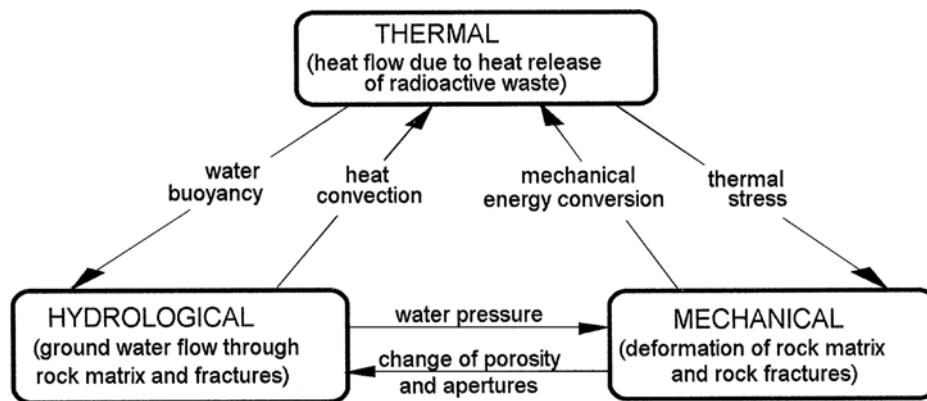


Figure 1. Coupled thermo-hydro-mechanical processes in a fractured rock [5].

from natural processes, such that transport of radioactive nuclides in the geosphere will be a very slow process and their eventual release to the biosphere will be in such low concentrations that they do not pose a hazard to human health and the natural environment. Performance assessment of nuclear waste repositories, either of the whole system or subsystems, is then needed to predict whether such isolation can be achieved [2].

What distinguishes a geological nuclear waste repository from other underground engineering facilities is its long designed life (from tens or even hundreds of thousands of years), well beyond that of any other rock engineering projects. For this kind of project, a high degree of design confidence is required [3]. In addition to the disturbances induced by repository excavation, thermal loading continuously disturbs the repository system. Key interactions between the rock masses and repositories (especially with placement of high-level nuclear wastes) include coupled phenomena involving thermal (T), hydrological (H), mechanical (M) and chemical (C) processes [4]. Coupled processes imply that one process affects the initiation and progress of another and that the behavior of a repository system cannot be predicted with confidence by considering each process independently (Figure 1) [5].

Considerable progress has been made in the study of coupled THM processes during the past two decades. A number of numerical codes have been developed to model the fully coupled THM processes of fractured rock masses and engineered barrier systems [6][7][8][9][10][11][12]. However, one of the remaining challenging tasks is to characterize the physical properties of the geological materials, especially the fractured hard crystalline rocks, with consideration of the effects of the fractures.

The existence of fractures makes the mechanical and hydraulic behaviors of fractured rock masses different from those of intact rocks. Fractures act often as major pathways for fluid flow, especially in hard rocks, and they make the overall mechanical behavior of the rock masses significantly different from the intact rocks. Further, nonlinear deformation of fractures makes the hydraulic and mechanical properties of fractured rock masses stress-dependent. Although numerical techniques exist to model the coupled hydraulic and mechanical behavior of fractured rock masses using discrete modeling approaches (e.g., [13]), the discrete approach is not practical for large scale problems (on the scale of kilometers) with extremely large numbers of fractures because of the limitation of computing power. Some studies implicitly consider fracture effects (e.g., [14]), however, this approach is limited in properly modeling the explicit geometry of fractures, the interactions among fractures and the

abrupt behavior of fractures such as shear dilation. Therefore, in large-scale analyses, a combination of the continuum approach and discrete approach at appropriate scales may be more effective in representing fracture effects on the behavior of fractured rock masses. In such an analysis, an equivalent continuum approach is used, with the equivalent properties derived using a discrete approach at smaller but representative scales, considering realistic fracture system geometry and physical behaviors of interacting fractures. In particular, change of permeability due to the change of stresses can be realistically determined using the discrete approach and the derived stress-permeability relations can be implemented into the continuum approach to better represent the hydromechanical behavior of fractured rock masses at a field scale.

This paper presents an equivalent continuum analysis of THM processes for a hypothetical repository (in this paper, it is confined to thermo-mechanical and hydro-mechanical processes due to thermal loading) with the equivalent properties determined from a discrete approach on fractured rock masses. Background information on site geology and fracture-system characterization was extracted from a site investigation programme of Nirex, at Sellafield, England [19]. The investigation was part of a benchmark test (BMT2) for the international co-operative research projects DECOVALEX III and BENCHPAR (with EU support). The objective of the BMT2 was to determine how the upscaling process impacts the performance assessment measures of a geological repository at a far-field scale [19]. Equivalent hydraulic and mechanical properties, the stress-dependent elastic modulus and stress-dependent permeability relation used for this paper are based on a series of previous works as the first stage of the same project [15][16][17][18].

The performance of the repository system is investigated in terms of mechanical responses and permeability changes induced by the thermal loading, caused by the heat releasing from nuclear waste decay as a function of time. Special focus is given to the sensitivity of coupled processes to mechanical properties. The large-scale problem is analyzed using a finite element method program, ROCKMAS (ROCK Mass Analysis Scheme [12]). The paper begins with the defined problem concerning a hypothetical geological repository, followed by an explanation of a discrete approach for determining equivalent properties, and the obtained results and conclusions.

2. Repository Model and Geological Data

2.1 The Generic Repository Model for the Analysis

In DECOVALEX III project, a benchmark test is established for understanding the impact of upscaling processes on performance assessment of a hypothetical nuclear waste repository defined [19]. A hypothetical reference problem is defined with simplifications of problem dimensions (2D instead of 3D) and of integrated fracture-system characterization of the Sellafield site and repository design. The geology is based on formations in the Borrowdale Volcanic Group, a thick sequence of Ordovician volcanoclastic rocks. The reference model is 5 km in width and 1 km in depth. Nuclear wastes were assumed to be uniformly placed within the repository of 10 m in height and 100 m in width (Figure 2) in size. The repository is assumed to comprise 60 canisters of wastes uniformly distributed over a horizontal repository area of 100 m x 100 m, embedded in compacted bentonite. No attempt is made to represent repository details such as drifts and deposition holes, and for simplicity, mechanical excavation effects are not considered. Tracking such effect would require proper 3D representations of the drift-hole system geometry and excavation steps. The large-scale model

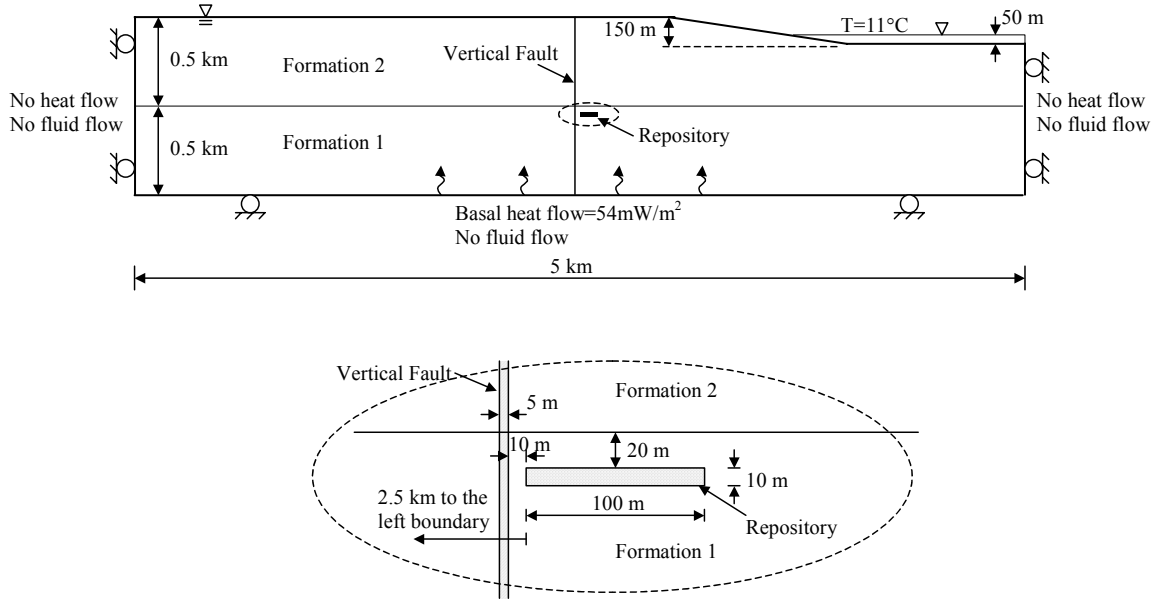


Figure 2. Reference model and boundary conditions for the Coupled THM analysis in far field (adapted from [19]).

Table 1. Model parameters used for the determination of equivalent properties and stress dependencies.

Parameter		
Intact rock	Elastic modulus (GPa)	84.6
	Poisson's ratio	0.24
Fractures	Dip/dip direction (4 sets)	8/145, 88/148, 76/21, 69/87
	Fisher constants (4 sets)	5.9, 9.0, 10.0, 10.0
	Fracture density per set (m ⁻²)	4.6*
	Normal stiffness (GPa/m)	434
	Shear stiffness (GPa/m)	434
	Cohesion (MPa)	0
	Friction angle (°)	24.9
	Dilation angle (°)	5
	Critical shear displacement for dilation, U _{cs} (mm)	3
	Joint Roughness Coefficient (JRC, scale 0.3 m)	3.85
	Joint wall compressive strength (MPa)	112.21
	Initial mechanical aperture at 1 st cycle (μm)	77
	Initial hydraulic aperture at 1 st cycle (μm)	65
	Initial aperture at 4 ^h cycle (μm)	30**
	Maximum aperture at 4 ^h cycle (μm)	50**
	Residual aperture at 4 ^h cycle (μm)	5**

*Fracture density is calculated from Eq. (1).

** No distinction was made between hydraulic and mechanical aperture.

is divided into two geological formations, with a vertical fracture zone cutting through both formations. The base and lateral sides of the model are no-flow boundaries and it is assumed that the water table is at the ground surface. The system was assumed to be fully saturated. The air temperatures at sea level and sea temperature are assumed to be constant at 11°C, for ground surfaces above sea level, the adiabatic lapse is 6.2°C /km. At the bottom of the model, a constant basal heat flux of 54 mW/m² is applied and no heat flux occurs on either lateral side of the model.

2.2 Geological Data

Geological data used for this study is listed in Table 1. For simplicity, these data are considered to be applicable to all geological formations. Note that the geological data sets are used merely for the reference-case example and are not intended to model the true characteristics of the site. In this regard, some parameters are selected in a simplified manner to determine the hydraulic and mechanical properties of fractured rock masses. Fracture data are based on the Coupled Shear Flow Tests (CSFT) of fractures samples, which measured the transmissivity changes during the closure and shearing of fractures [19].

Four fracture sets are identified and the length of fracture follows a power law as follows.

$$N = 4 \times L^{-D} \quad (1)$$

where D is the fitted fractal dimension equal to 2.2 ± 0.2 , with the value 2.2 used for this study. The relation in Equation (1) was obtained from combined analysis of aerial photography lineaments and mapping results from scan-line data and outcrop trace mappings [19]. For this study, the minimum and maximum cut-offs of trace-lengths are set to be 0.5 m and 250 m, respectively. Figure 3 shows the fractal nature of fracture trace-length distribution as fitted by Equation (1).

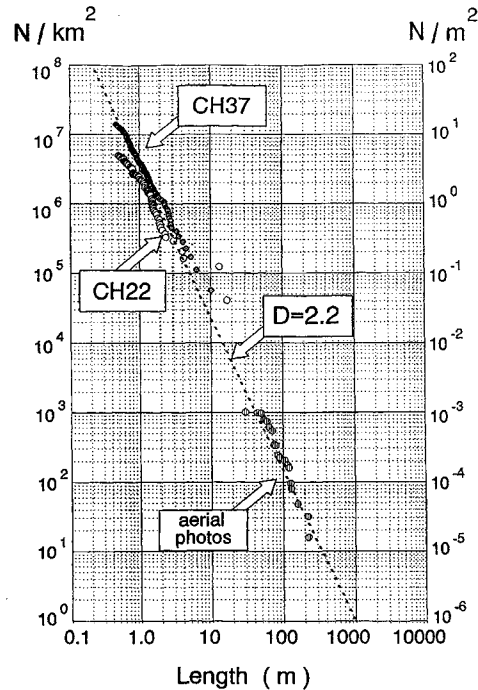


Figure 3. Plot of length against number per km² for surface mapping sites CH22 and CH37, and for long fracture samples from the photolineament. Data fall on a line establishing a power-law scaling relationship for trace-length in the range of 0.5 to 250 m [20].

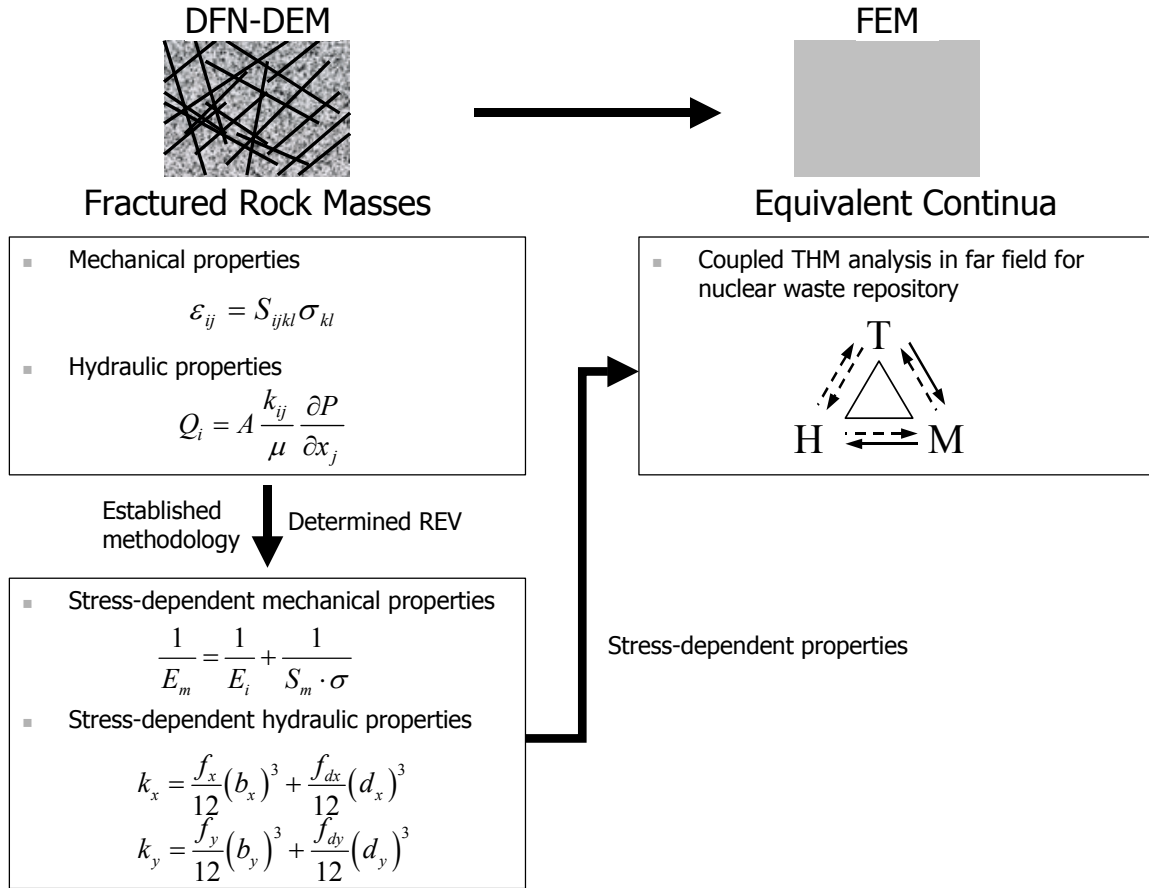


Figure 4. Conceptual approach of the coupled THM analysis of equivalent continuum. Thermo-mechanical and hydro-mechanical processes are considered in this study (indicated as solid line in T-H-M diagram).

3. Methodology

3.1 Determination of Equivalent Properties

The conceptual approach adopted for this study is displayed in Figure 4. In this study, fractured rock masses are treated as equivalent continua. A series of numerical experiments were conducted to determine the hydraulic and mechanical properties of fractured rock masses and their stress dependencies, using a hybrid DFN-DEM (discrete fracture network-distinct element method) approach [15][16][17][18]. The DFN-DEM approach uses the fracture system realizations as the geometric models of the fractured rock masses and conduct numerical experiments using DEM for the calculation of mechanical and hydraulic properties. Multiple DFN realizations were generated independently to represent the geometry models of fractured rock masses and they are passed on to a DEM program, UDEC [13] for the numerical experiments.

A series of numerical experiments were conducted to investigate the existence of representative elementary volume (REV) and the existence of properly defined tensor property in the decided REV sizes [15][16], using two criteria defined to determine the sizes of REV according to required resolutions. For this study, the REV size of 5 m × 5 m was established as adequate representative REV and was used for the additional numerical experiments investigating the effect of stresses on mechanical properties and permeability [17][18]. By conducting mechanical and hydraulic tests at different stress levels, we were able

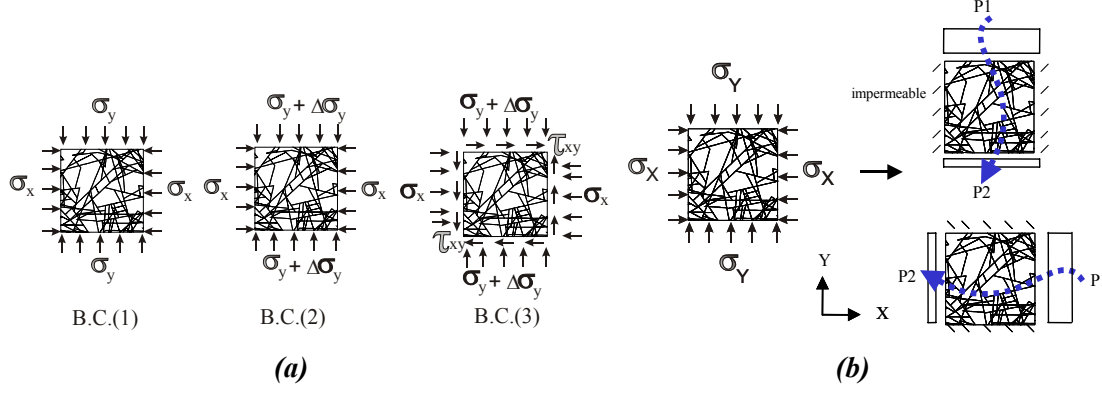


Figure 5. Boundary conditions for the determination of (a) mechanical properties, and (b) stress-dependent permeability of fractured rock masses [15][18].

Table 2. Parameters determined from numerical experiments [21]. The scale of the models are 5 m × 5 m.

Determined properties from DFN-DEM numerical experiments	
Mechanical Properties expressed in compliance matrix (constant stiffness)	
$\text{model}) \begin{pmatrix} S_{11} & S_{12} & S_{13} & S_{16} \\ S_{21} & S_{22} & S_{23} & S_{26} \\ S_{31} & S_{32} & S_{33} & S_{36} \\ S_{61} & S_{62} & S_{63} & S_{66} \end{pmatrix} = \begin{pmatrix} 2.7772 & -0.2946 & -0.2801 & -0.0446 \\ -0.2927 & 2.3914 & -0.2816 & -0.0451 \\ -0.2801 & -0.2816 & 1.1820 & -0.0048 \\ -0.0584 & -0.0639 & -0.0048 & 5.5654 \end{pmatrix} \times 10^{-2} (1/\text{GPa})$	Mean of ten models
Permeability (constant aperture, 65 μm)	
$\begin{pmatrix} k_{xx} & k_{xy} \\ k_{yx} & k_{yy} \end{pmatrix} = \begin{pmatrix} 1.0384 & 0.0393 \\ 0.0393 & 1.3258 \end{pmatrix} \times 10^{-13} (m^2)$	Mean of ten models
Stress-dependent Mechanical properties	
$\frac{1}{E_m} = \frac{1}{E_i} + \frac{1}{S_m \cdot \sigma}$	Fitted curve from ten models
Sensitivity parameter (S_m)	1859.9
Poisson's ratio	0.6 – 0.85
Stress-dependent permeability	
$k_x = \frac{f_x}{12} \left[b_r + b_{\max} \exp\{-(\alpha_x \sigma_x + \alpha_y \sigma_y)\} \right]^3 + \frac{f_{dx}}{12} \left[d_{\max} \left[1 - \exp\{-\gamma_x (k - k_c)\} \right] \right]^3$	Determined from one model
$k_y = \frac{f_y}{12} \left[b_r + b_{\max} \exp\{-(\beta_x \sigma_x + \beta_y \sigma_y)\} \right]^3 + \frac{f_{dy}}{12} \left[d_{\max} \left[1 - \exp\{-\gamma_y (k - k_c)\} \right] \right]^3$	
Equivalent frequency (f_x)	4.44 (1/m)
Equivalent frequency (f_y)	5.11 (1/m)
Stress coefficient (α_x, α_y) for b_x	0.034, 0.146
Stress coefficient (β_x, β_y) for b_y	0.101, 0.071
Equivalent dilation frequency (f_{dx}, f_{dy})	0.384, 0.046 (1/m)
Stress coefficient (γ_x and γ_y) for dilation d_x and d_y	1.88, 1.95
Critical stress ratio (k_c)	2.45

to construct a set of empirical equations that account for the effect of stress. Figure 5 shows the necessary boundary conditions for the determination of mechanical properties and stress dependent permeability used in the UDEC simulations. The results for the equivalent mechanical and hydraulic properties are listed in Table 2 at corresponding stages of calculations.

Finally, the mechanical and hydraulic properties corresponding to different stress levels with depth were passed on to the large-scale model to examine the impacts of thermo-mechanical processes on the performance assessment of a hypothetical nuclear waste geological repository.

3.2 Modeling Methodology at the Large Scale

The large-scale analysis is conducted based on the defined geometry of a hypothetical repository, with initial and boundary conditions as defined in the benchmark test (Figure 2). Heat decay data are taken from a typical example [22] and Figure 6 shows the heat evolution after emplacement of the nuclear wastes. Heat evolution is modeled by the following equation

$$\begin{aligned} flux(W) &= 1000, \quad x \leq 10, \quad x = year \\ flux &= 10^{(-0.3979 \log_{10} x + 3.3979)}, \quad x \geq 10 \end{aligned} \quad (2)$$

The thermal gradient for the *in situ* condition was calculated to be about 2.4 (°C/100 m).

The *in situ* stress data are from Sellafield area and are slightly modified for modeling purposes (assigning a zero-stress condition at the top of the model). The modified vertical and horizontal *in situ* stresses are functions of depths, D, as follows

$$\begin{aligned} \sigma_{ver} &= -0.02520622 \cdot D \\ \sigma_{hor} &= -0.0331747 \cdot D \end{aligned} \quad (3)$$

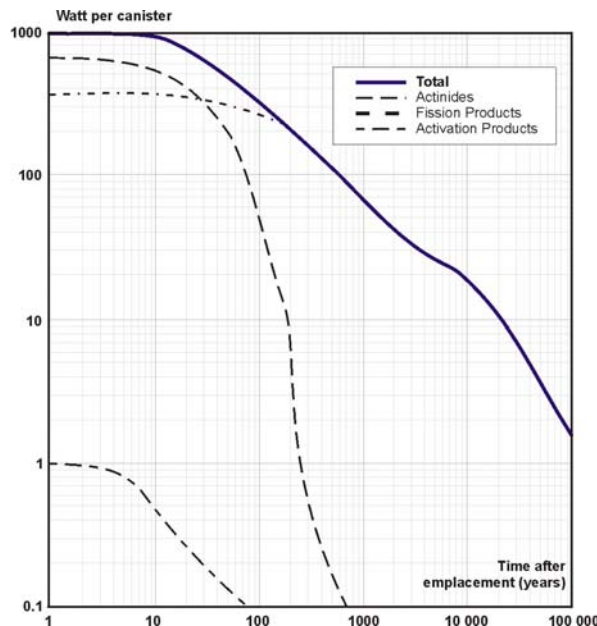


Figure 6. Heat evolution versus time for a single canister [22].

Table 3. Input parameters for large-scale analysis. Each unit is equally divided into bottom and upper part.

Properties	F1 (bottom)	F1 (upper)	F2 (bottom)	F2 (upper)	Repository (Bentonite)***
Elastic modulus*(GPa)					
Case 1	23.01	17.69	11.81	3.88	17.69
Case 2	39.0	39.0	39.0	39.0	39.0
Case 3	84.6	84.6	84.6	84.6	84.6
Poisson ratio*					
Case 1	0.45	0.45	0.45	0.45	0.45
Case 2	0.11	0.11	0.11	0.11	0.11
Case 3	0.24	0.24	0.24	0.24	0.24
Permeability (m ²)*					
k _{xx}	1.17e-16	2.62e-16	8.14e-16	4.40e-15	1e-20
k _{yy}	1.05e-16	2.22e-16	7.13e-16	4.56e-15	1e-20
Coefficient of thermal expansion**	0.1e-4	0.1e-4	0.1e-4	0.1e-4	0.1e-4
Solid heat capacity (J/kg/K)	0.798e+3	0.798e+3	0.798e+3	0.798e+3	0.871e+3
Solid-fluid mixture thermal conductivity (W/mK)	0.229e+1	0.229e+1	0.229e+1	0.229e+1	0.13e+1
Density (kg/m ³)	2.52 × 10 ³	1.6 × 10 ³			

*: *Elastic modulus, poisson ratio and permeability values are based on upscaling with DFN-DEM analysis.*

** : *Typical values are used*

***: *Bentonite: mechanical and hydromechanical properties of bentonite is not explicitly modeled.*

The ratio of maximum horizontal stress to vertical stress is about 1.3. The displacements on both lateral sides and at the bottom of the model are constrained in the lateral (x-direction) and vertical direction (y-direction), respectively, with the plane strain condition. According to the definition of the generic benchmark test problem, the initial fluid flow is expected to be driven by the topography.

Table 3 shows the input parameters used for the large-scale analysis of the repository model. In this study, two formations (Formation 1 and 2) are subdivided into two layers of equal thickness, F1 (bottom), F1 (upper), F2 (bottom) and F2 (upper) in Table 3, and the corresponding depth (i.e., stress) is considered when assigning the mechanical and hydraulic properties. The properties of fault are also selected at corresponding depth without distinguishing them from the other two formations.

To investigate the effect of different methods of determining the properties, three cases (Case 1, Case 2 and Case 3) are considered, whose values differ only in their mechanical properties. Case 1 is the base case, in which stress-dependent elastic modulus were derived from the hybrid DFN-DEM approach using the UDEC code. The elastic modulus varies with

depth and a constant Poisson’s ratio was used. Since the anisotropy of elastic modulus was not high, isotropy was assumed. Even though Poisson’s ratio calculated from the DFN-DEM approach is very high (0.6 –0.85), above the limit of the isotropic case (0.5), a value less than upper limit of isotropic case (0.45) is chosen, since the mechanical properties are assumed to be isotropic. Case 2 uses mechanical properties based on the constant stiffness of fractures and both elastic modulus and Poisson’s ratio are lower than that of intact rock. Case 3 simply uses the mechanical properties of intact rock without any consideration of the role of fractures. Permeability are identical in all three cases.

Figure 7 shows the generated mesh for the large scale model. The element size is chosen to be larger than the determined REV size of 5 m by 5 m.

3.3 Numerical Code Description

For the large-scale analysis, the ROCMAS code is used. ROCMAS is a finite-element code developed for analysis of coupled THM processes in saturated-unsaturated fractured porous media [12]. The original formulation of coupled thermohydroelasticity in terms of Biot's theory of consolidation [23] is extended to partially saturated media for heat and moisture flow [12]. In the formulation of ROCMAS, three balance equations—water mass balance, energy conservation and linear momentum balance—and a number of constitutive relations are required for a full description of the THM states, leading to a set of governing equations. Detailed descriptions can be found in [12]. ROCMAS has been applied in a number of different applications such as heating tests, tunnel excavations, a flow injection test and modeling the performance of a nuclear waste repository [6][24][25][26][27]. In this study, thermo-mechanical analysis is conducted without considering thermo-hydraulic coupling, with the focus placed on the impact of thermal loading on mechanical response and permeability change.

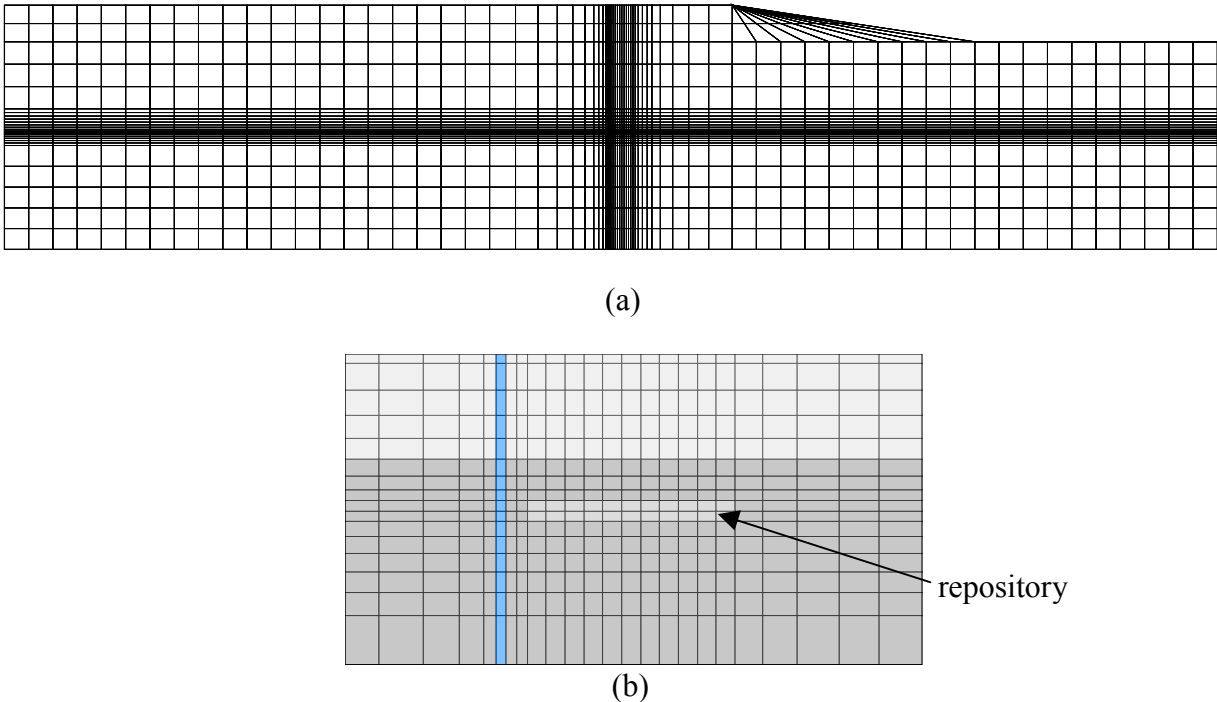


Figure 7. Mesh for the FEM analysis. (a) entire model, (b) detailed view around the repository.

4. Repository scale Thermo-Mechanical Analysis

4.1 Temperature Distributions

Figure 8 shows the temperature distributions at different time. A maximum temperature of about 50°C occurs at about 100 years after the waste placement. Because of the continuous decay of the waste, the maximum temperature continues to decrease with time and the influence area of temperature becomes bigger (e.g., along the vertical or horizontal reference lines in Figure 9) with the increase of time as shown in Figure 10.

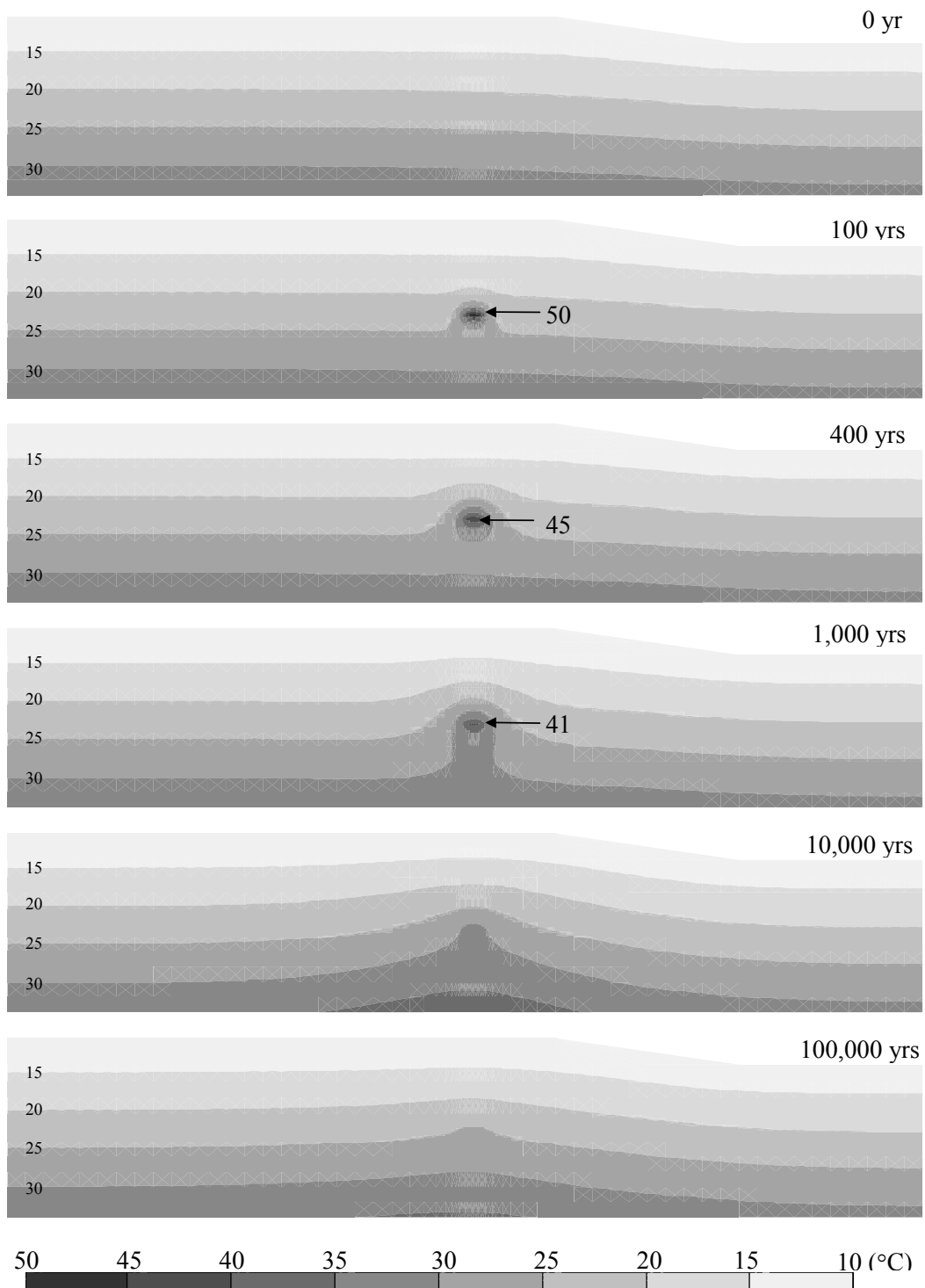


Figure 8. Temperature distributions at different time scales.

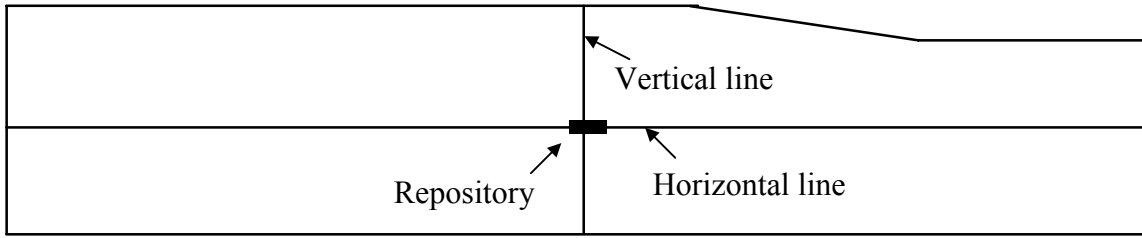


Figure 9. Location of reference lines across the repository.

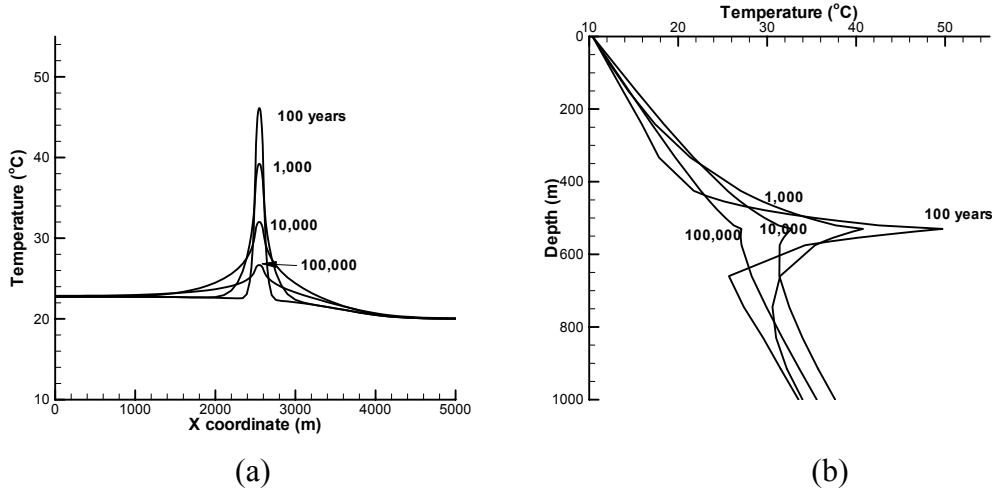
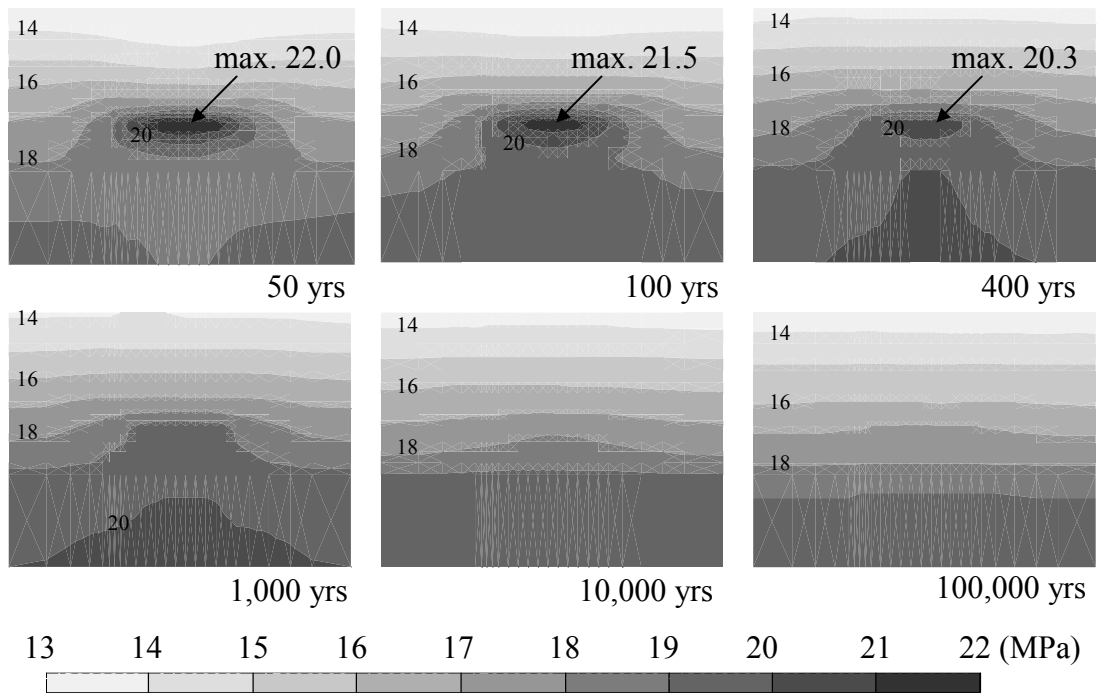


Figure 10. Temperature distribution at different time scales. (a) along the horizontal line, (b) along the vertical line.

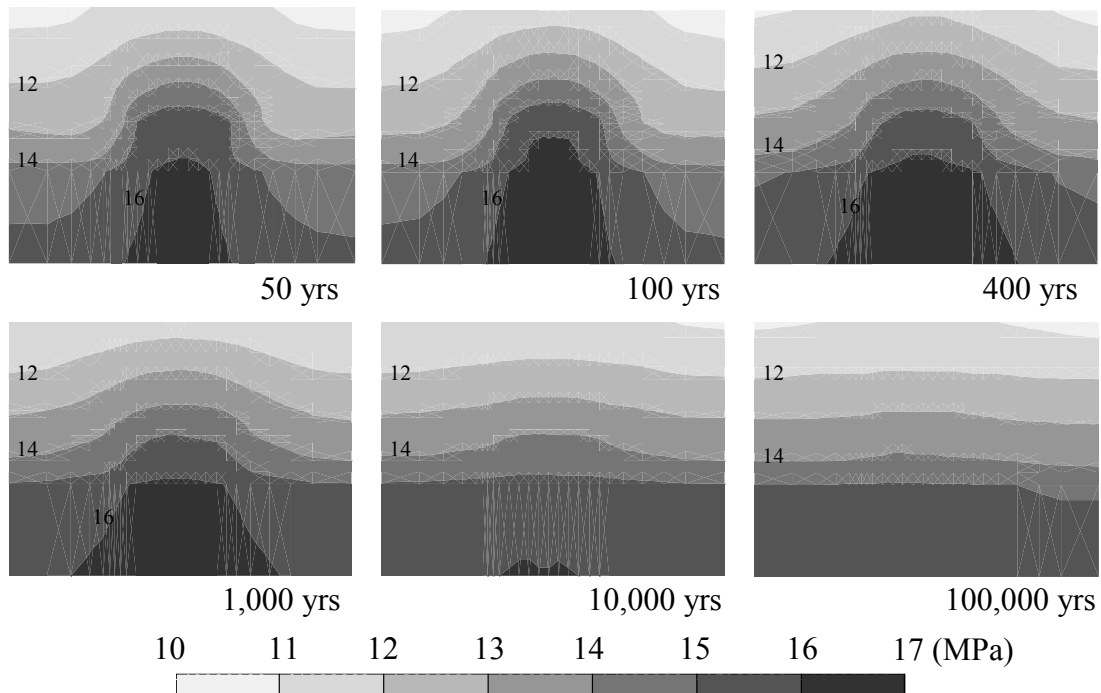
4.2 Stress and Displacement Distributions

Stresses and displacements induced by the thermal disturbance are investigated. Figure 11 shows the stress (*in situ* stress plus thermal stress) distributions at different time. The maximum contribution from the thermal stress was about 5 MPa at about 100 years time, corresponding to the peak temperature. Because the ground surface is free to move, the thermal stresses in the y-direction are smaller than that in the x-direction. Stresses in horizontal and vertical reference lines (see in Figure 9) are shown in Figure 12.

Since the thermal stress is highly dependent on the deformation characteristics of the rock, the three cases introduced above are compared. Figure 13 shows the horizontal thermal stresses in horizontal and vertical reference lines across the repository. As can be seen, induced thermal stresses vary greatly with the mechanical properties. When only the intact rock properties were used (Case 3), the maximum thermal stress in the horizontal direction was nearly 20 MPa, whereas it is only 5 MPa when the effect of fractures was considered through equivalent mechanical properties (Figure 13a and Figure 13b). Such a difference can also be observed for the horizontal thermal stresses at different time in Figure 13c and Figure 13d. What is interesting is the generated tensile stress in the surface. The induced tensile stress is small in Case 1, however, much bigger tensile stress is induced in Case 3 (about 3 MPa at 1,000 years). This large difference is due to the large difference of elastic modulus near the surface. Note that the elastic modulus was 3.88 MPa for Case 1 and 84.6 MPa for Case 3 in upper zone of Formation 2. A similar tensile zone was also found in [28] where tensile stress was generated in the surface above the repository. Since rock is very weak for tensile strength, this observation needs to be further investigated for the performance assessment of the repository system.



(a)



(b)

Figure 11. Stress distribution at different time scales (Case 1). (a) x-directional normal stress, (b) y-directional normal stress.

Figure 14 shows the vertical displacement distributions over time. The general trend shows a heaving of rock above the repository, of a few centimeters. This magnitude of displacement may or may not cause safety concerns at the ground surface. However, analysis may be needed for confidence-building measures, such as post-closure monitoring. On account of the slow diffusion of thermal processes, maximum displacement is observed at about 10,000

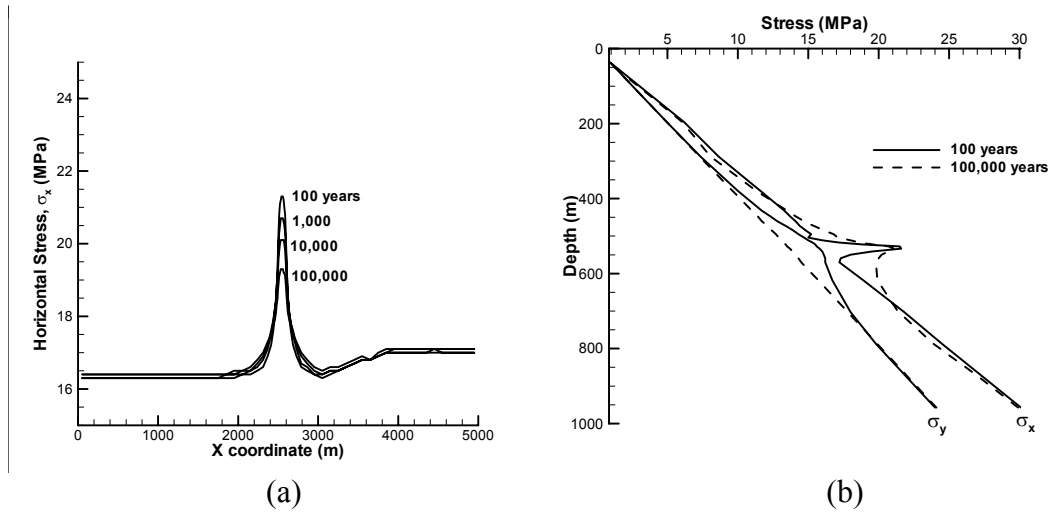


Figure 12. Stress distributions at different time scales (Case 1). (a) Horizontal stress along the horizontal reference line, (b) Vertical and horizontal stresses along the vertical reference line.

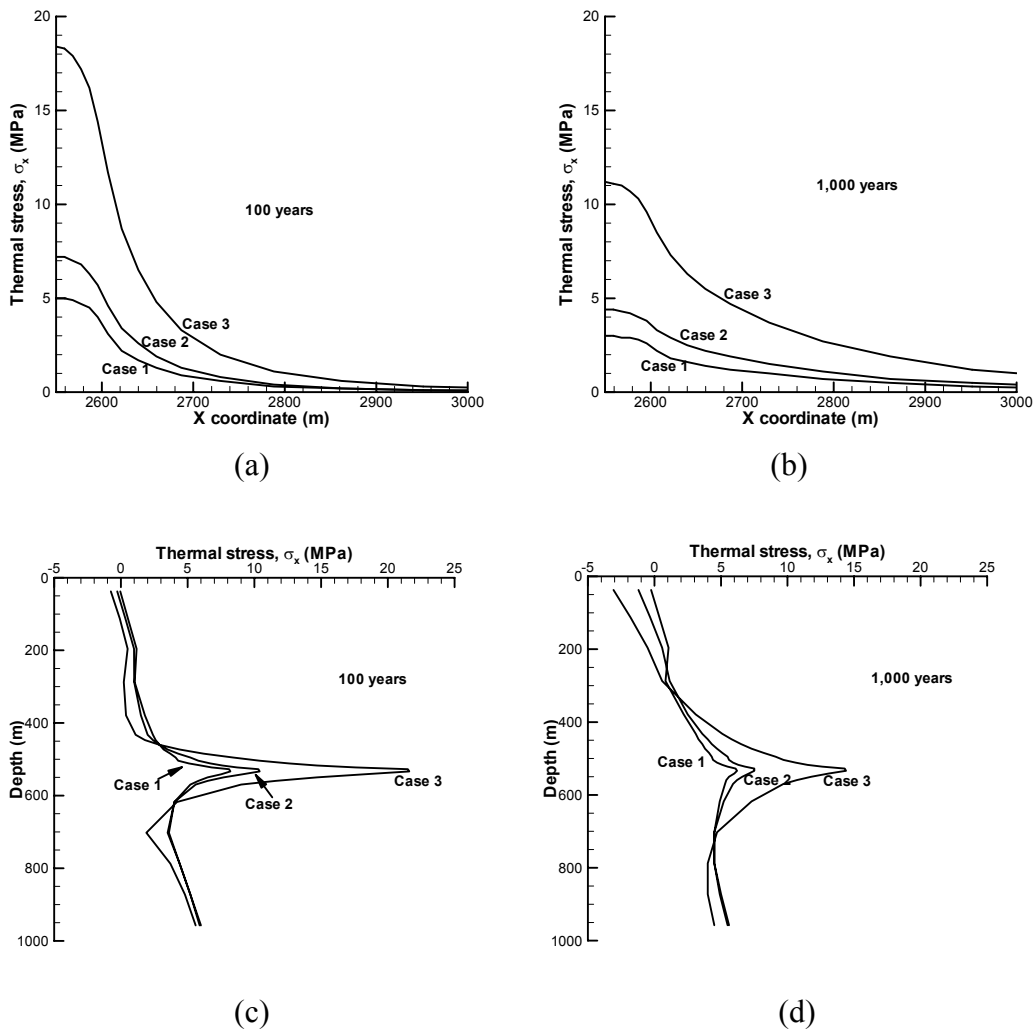


Figure 13. Horizontal thermal stresses in different cases. (a) Along horizontal reference line in 100 years, (b) Along horizontal reference line in 1,000 years, (c) Along vertical reference line in 100 years, (d) Along vertical reference line in 1,000 years.

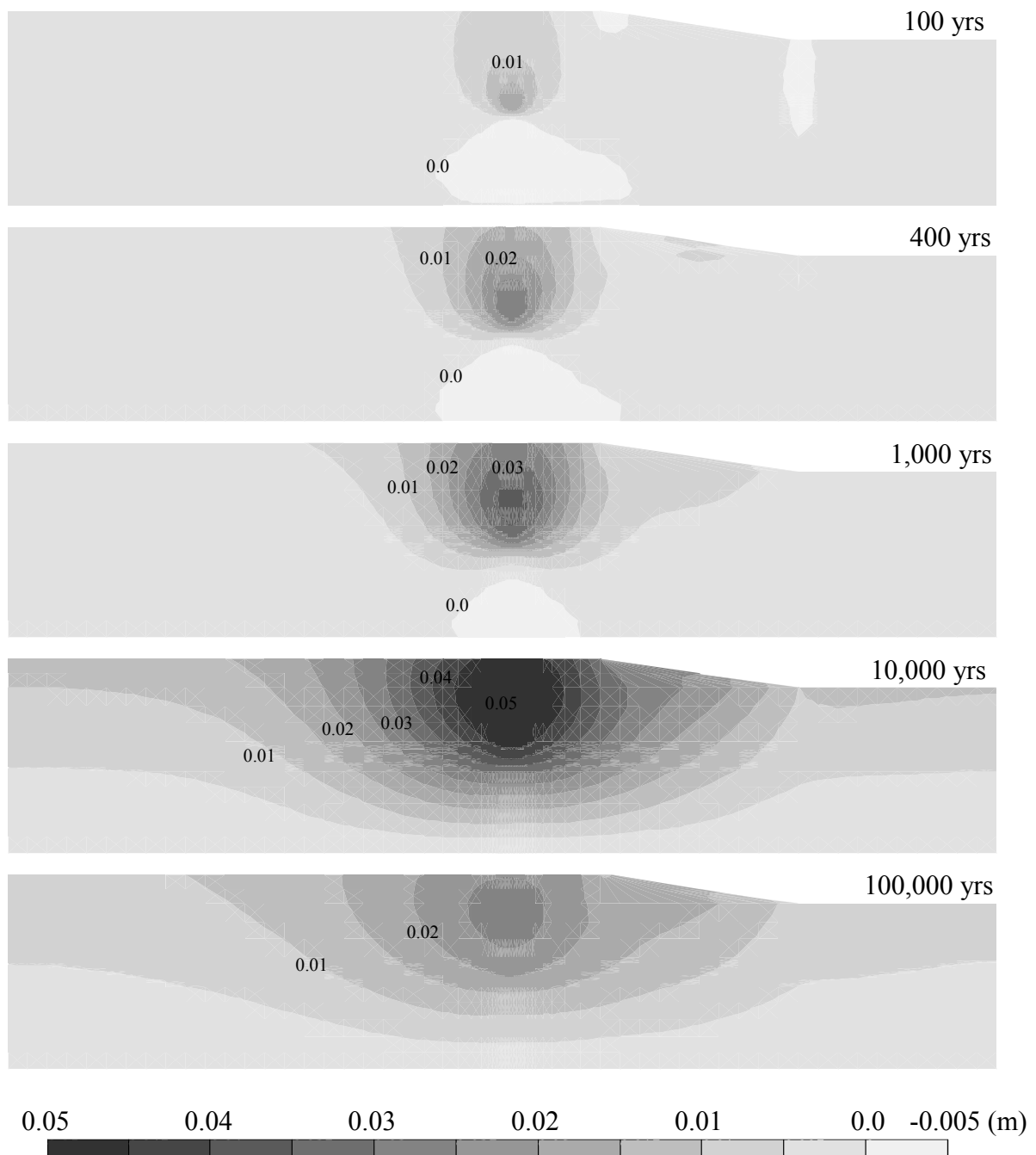


Figure 14. Vertical displacement distribution at different time scales (Case 1).

years. After this period, the heaved ground settles with the decreased temperature. The location of maximum displacement shifts from directly above the repository (e.g., at 10 years) upward as time passes (Figure 15).

The displacement field also depends on mechanical properties - the results of three different cases are shown in Figure 16. Case 1, in which the elastic modulus is small and Poisson's ratio is large, has the largest displacement. Case 2, in which the elastic modulus is moderate and Poisson's ratio is small, has the smallest displacement. The difference in displacement is caused mainly by the differing Poisson's ratios, since the thermal expansion

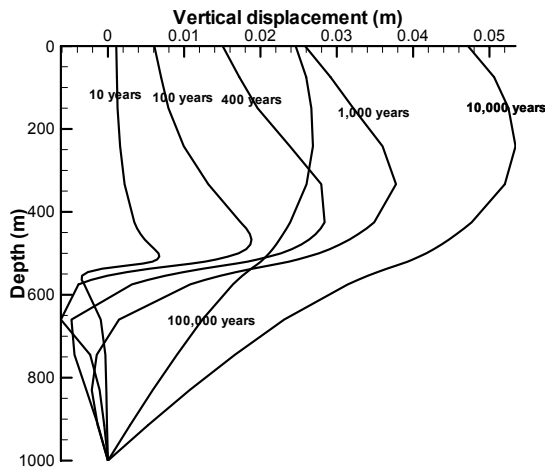


Figure 15. Vertical displacement along the vertical line at different time (Case 1).

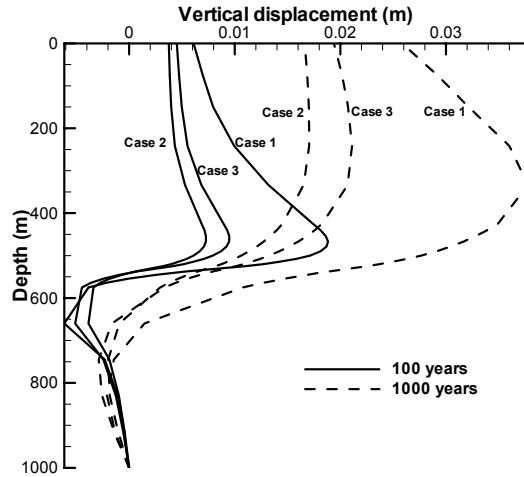


Figure 16. vertical displacements along vertical line at different cases of mechanical properties of rocks.

coefficients are the same in all three cases. When the Poisson's ratio is high, the heaving becomes large, owing to confined lateral boundaries.

Horizontal displacement distributions over time are shown in Figure 17. As was indicated in [25], a zone of tensile displacement is generated above the repository resulting from rock expansion. This tensile displacement has to be further investigated with the observed tensile stress.

The results of stress and displacement fields show the importance of properly determining the mechanical properties of the fractured rock masses for the thermo-mechanical analysis.

5. Permeability Change Caused by Thermal Stress

Using the stress-dependent permeability equations established in previous studies (Table 2), the permeability changes induced by the thermal stress are investigated. Figure 18 shows the permeability change distributions at different time. The changed permeability is normalized with respect to the permeability at the initial effective stress state. The magnitudes of changed permeability increased from 100 years to 1,000 years and then becomes smaller again at 10,000 years. The permeability generally decreases owing to the induced compressive stresses around the repository, with the magnitude of normalized permeability less than 0.5. Empirical equations of stress-dependent permeability (Table 2) indicate that the shear dilation of fractures plays a significant role in the increase of permeability. However, no dilation was induced from the thermal loading in this study. The stress ratio (the ratio of horizontal stress to vertical stress) in this study was about 1.3. When the stress is expressed in terms of effective stress, the ratio is about 1.5. Even though the thermal stress component has a greater increase in the horizontal direction, the addition of thermal stress was not substantial enough to reach the critical stress ratio (about 2.45 for conditions in this study). However, if the *in situ* stress state is close to this critical stress, even a slight contribution from the thermal stress can give rise to the onset of shear dilation. This possibility has to be considered when selecting a site for a nuclear waste repository. Furthermore, this relative smaller change even

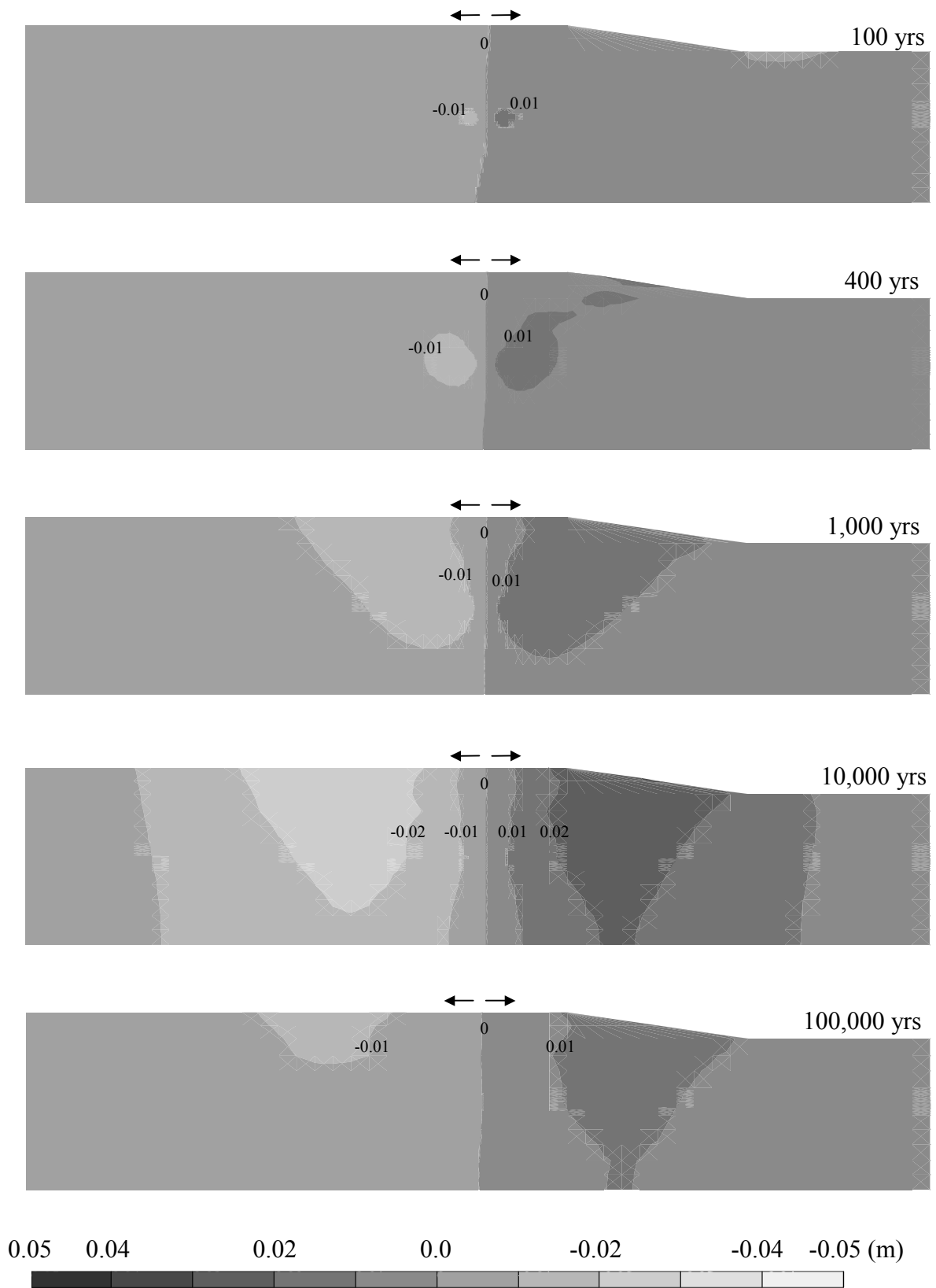
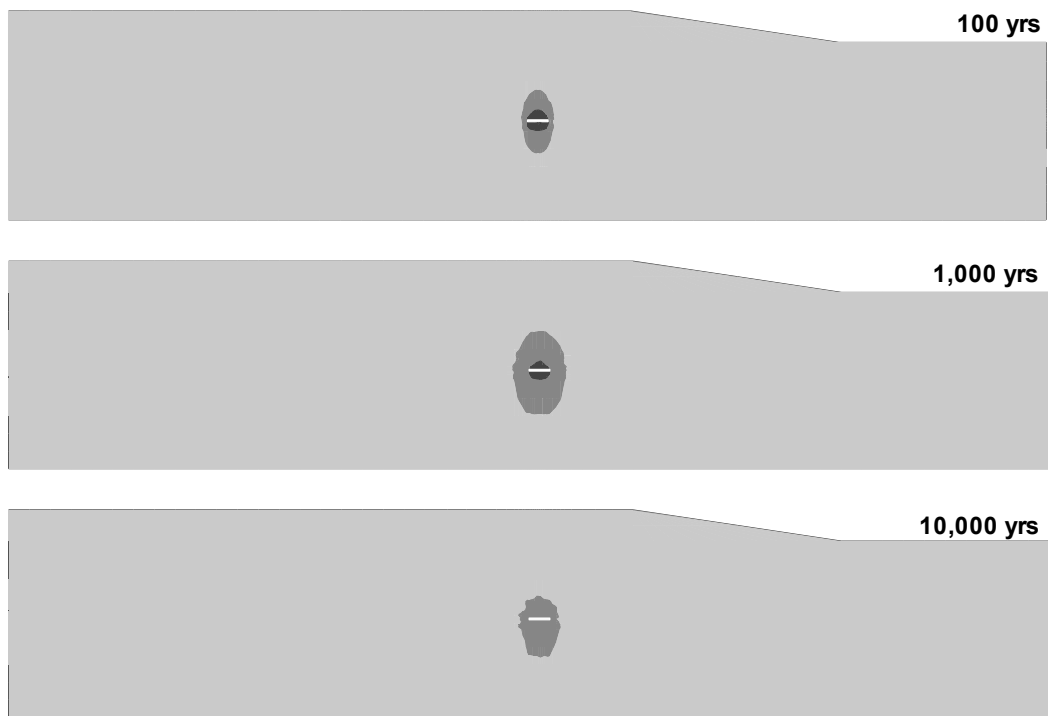
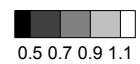
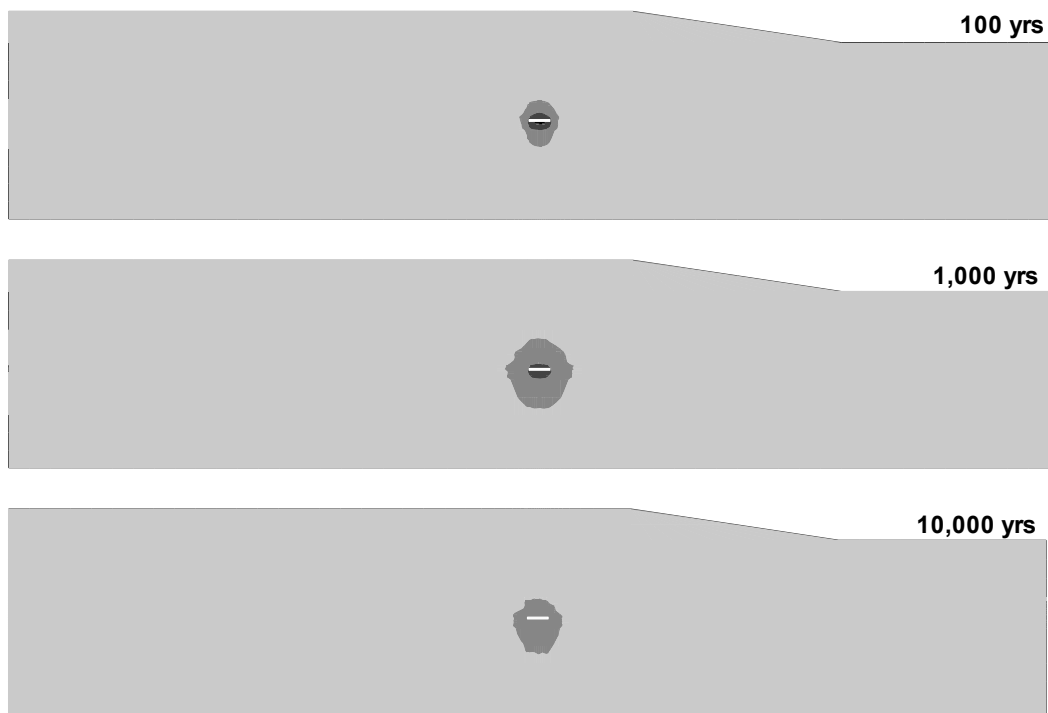


Figure 17. horizontal displacement distributions at different time scale (Case 1).



(a)



(b)

Figure 18. Permeability change due to the induced thermal stress (Case 1). Permeability is normalized with respect to the initial permeability (a) normalized horizontal permeability (b) normalized vertical permeability.

around the repository largely results from the mechanical excavation effect not being considered in this study. Further work regarding the validity of the stress-permeability relation and the application of it to the large scale heating problem, with a proper presentation of repository geometry and excavation sequence, need to be done for more realistic estimation of thermo-mechanical effect on permeability change.

6. Conclusions

In this study, coupled THM processes in a nuclear waste repository in fractured rock masses were numerically investigated by an equivalent continuum approach at a far-field scale. The main performance measures were mechanical response and permeability change induced by thermal loading. Our conclusions are as follows:

A combined discrete and continuum modeling approach is presented. The procedures for determining the equivalent mechanical and hydraulic properties of fractured rock masses are introduced, with their stress-dependencies applied as input data for the large-scale analysis. This methodology provides a more systematic platform for large-scale engineering applications in fractured rock masses, such as a geological repository of nuclear waste.

The responses of fractured rock masses vary significantly according to how mechanical properties are determined, which may have significant consequences for the performance of the repository. The results from the three cases in this paper show significant differences in stresses and displacements between simply-assumed mechanical properties and systematically determined equivalent properties. One special issue raised by the results of this paper is the differences in thermal stresses when properly derived equivalent mechanical properties and intact rock properties are used. For repositories in intact or extremely sparsely fractured hard rocks, the thermal stress increment will be very significant in terms of repository safety. In fractured rocks, this safety concern has much less significance.

The calculated results also show the development of vertical heaving and horizontal tensile displacements, which may be important issues for confidence-building and the performance assessment of repository systems. Observed displacement fields also depend on how the mechanical properties (i.e., elastic modulus and Poisson's ratio) are characterized considering the effects of fractured systems.

Coupled effects were investigated considering the permeability changes induced by thermo-mechanical processes. Permeability changes induced by thermal loading indicate that they generally decreased by a factor of two close to the repository. Thermally induced fracture dilation was not observed. Permeability change on the large scale seems to be small and the effects diminish over time. However, this conclusion has to be interpreted carefully in relation to the role of *in situ* stress conditions, and to the assumptions that did not consider excavation effects. With excavation properly simulated, the effects may be more significant, especially near the repository, and could have an impact on design, construction and operation of the repository and post-closure monitoring. This effect needs to be included for more realistic simulations of the rock-mass responses, more properly in three dimensions.

The current study focuses on thermo-mechanical impacts. However, full thermo-hydro-mechanical and radionuclide transport analysis needs to be conducted for more complete assessment of performance for the geological repository.

Acknowledgements

The financial support by the European Commission through the BENCHPAR Project (FIKW-CT-2000-00066) and the Swedish Nuclear Inspectorate (SKI) through the DECOVALEX III Project are gratefully acknowledged.

7. Reference

- [1] Witherspoon, PA, Introduction to second world wide review of geological problems in radioactive waste isolation, *Geological Problems in Radioactive Waste Isolation*, LBNL-38915, UC-814, 1996:1-4
- [2] International Atomic Energy Agency, Scientific and Technical Basis for the Geological Disposal of Radioactive Wastes, Technical Report Series No. 413, IAEA, Vienna, 2003
- [3] Hudson JA, Stephansson O, Andersson J, Tsang CF, Jing L, Coupled T-H-M issues relating to radioactive waste repository design and performance, *Int J Rock Mech Min Sci* 2001;38(1):143-61
- [4] Tsang CF, Coupled processes associated with nuclear waste repositories, Academic Press, New York, 1987
- [5] Jing L, Tsang CF, Stephansson O, DECOVALEX - An International Co-Operative Research Project on Mathematical Models of Coupled THM Processes for Safety Analysis of Radioactive Waste Repositories, *Int J Rock Mech Min Sci* 1995;32(5):389-98
- [6] Noorishad J, Tsang CF, Witherspoon PA, Coupled Thermal-Hydraulic-Mechanical Phenomena in Saturated Fractured Porous Rocks: Numerical Approach, *J Geophys Res* 1984;89(B12):10365-73
- [7] Hart RD, St John CM, Formulation of a fully-coupled thermal-mechanical-fluid flow model for non-linear geologic systems, *Int. J. Rock Mech. Min. Sci. & Geomech. Abstr.*, 1986;23(3):213-24.
- [8] Ohnishi Y, Kobayashi A, Thermal-Hydraulic-Mechanical Coupling Analysis of Rock Mass, In:Hudson JA (eds), *Comprehensive Rock Engineering*;Vol.2:191-208
- [9] Nguyen TS and Selvadurai APS, Coupled thermal-mechanical-hydrological behaviour of sparsely fractured rock: Implications for nuclear fuel waste disposal, *Int J Rock Mech Min Sci* 1995;32(5):465-79
- [10] Bower KM, Zyvoloski G, A numerical model for thermo-hydro-mechanical coupling in fractured rock, *Int J Rock Mech Min Sci* 1997;34:1201-11
- [11] Stephansson, O., Jing, L., and Tsang, CF (eds). *Coupled Thermo-hydro-mechanical Processes of Fractured Media*. Developments in Geotechnical Engineering, Elsevier. 79. Amsterdam:Elsevier, 1996
- [12] Rutqvist J., Børgesson L., Chijimatsu M., Kobayashi A., Nguyen TS., Jing L., Noorishad J., and Tsang CF 2001, Thermohydromechanics of partially saturated geological media: governing equations and formulation of four finite element models. *Int. J. Rock mech. Min. Sci.* 38(1), 105-27
- [13] Itasca Consulting Group, *UDEC user's guide*, Ver. 3.1, Minnesota, 2000.
- [14] Sasaki T, Morikawa S, Thermo-mechanical consolidation coupling analysis on jointed rock mass by the finite element method, *Eng Computation* 1996;13(7):70-86.
- [15] Min KB, Jing L, Numerical determination of the equivalent elastic compliance tensor for fractured rock masses using the distinct element method, *Int J Rock Mech Min Sci* 2003;40(6):795-816
- [16] Min KB, Jing L, Stephansson O, Determining the Equivalent Permeability Tensor for Fractured Rock Masses Using a Stochastic REV Approach: Method and Application to the Field Data from Sellafield, UK, *Hydrogeology Journal* (in press)

- [17] Min KB, Jing L, 2004, Stress dependent mechanical properties and bounds of Poisson's ratio for fractured rock masses investigated by a DFN-DEM technique, *Int J Rock Mech Min Sci*;41(3):431-2
- [18] Min KB, Rutqvist J, Tsang CF, Jing L, Stress-dependent permeability of fractured rock masses: a numerical study, *Int J Rock Mech Min Sci*; (submitted)
- [19] Anderson J, Knight L, DECOVALEXIII Project, TASK 3, BMT2 protocol, Understanding the Impact of Upscaling THM processes on Performance Assessment, version 6.0, Stockholm, 2000 (unpublished report)
- [20] Nirex, Evaluation of Heterogeneity and Scaling of Fractures in the Borrowdale Volcanic Group in the Sellafield Area, Nirex Report SA/97/028, 1997
- [21] Min KB, Jing L, Understanding the impact of Upscaling on the THM processes on Performance Assessment, Decovalex III Task3, BMT2, SKI report, 2004 (in preparation)
- [22] SKB, SR 95 Template for safety reports with descriptive example, SKB Technical Report TR 96-05, Stockholm, 1996
- [23] Biot M. A., General Theory of Three-Dimensional Consolidation, *J. Appl. Phys.* 1941;12:155-64
- [24] Noorishad J, Tsang CF, Witherspoon PA, 1992, Theoretical and field studies of coupled hydromechanical behaviour of fractured rocks – 1. Development and verification of a numerical simulator, *Int J Rock Mech Min Sci* 1992;29(4):401-9
- [25] Noorishad, J., and Tsang, CF, Coupled Thermoelasticity Phenomena in Variably Saturated Fractured Porous Rocks - Formulation and Numerical Solution, In: Stephansson, O., Jing, L., and Tsang, CF (eds). *Coupled Thermo-hydro-mechanical Processes of Fractured Media*. Developments in Geotechnical Engineering, Elsevier. 79;1996:93-134
- [26] Rutqvist J, Noorishad J, Stephansson O, Tsang CF, Theoretical and Field Studies of Coupled Hydromechanical Behaviour of Fractured Rocks – 2. Field Experiment and Modelling, *Int J Rock Mech Min Sci* 1992;29(4):411-19
- [27] Rutqvist J, Börgesson L, Chijimatsu M, Nguyen TS, Jing L, Noorishad J, and Tsang CF. 2001 Coupled Thermo-hydro-mechanical analysis of a heater test in fractured rock and bentonite at Kamaishi Mine – comparison of field results to predictions of four finite element Codes. *Int. J Rock mech Min Sc.* 38(1), 129-42
- [28] Liu H-H, Zhou Q, Rutqvist J, Bodvarsson B, Understanding the Impact of Upscaling THM Processes on Performance Assessment (DECOVALEX III BMT2), unpublished report